1 生体内鉄代謝の機構

生田克哉，高後　裕　旭川医科大学 内科学講座 消化器・血液腫瘍制御内科学分野

生体内鉄代謝の概要

鉄は生体内に存在する金属元素のうち，最も多く存在するものである．最も多くの鉄は赤血球中のヘモグロビン（Hb）の成分として使用され，全身への酸素の運搬に機能しているが，その他にも全身の細胞の分裂や増殖，様々な代謝などに必要不可欠である．しかし，いくら必要不可欠な鉄とは言っても，逆に過剰に存在してしまうと，細胞に対して毒性を示してしまうため，生体内において鉄代謝は巧妙に制御される必要がある[1]．

生体における鉄動態を吸収から見ていくと，**図1**に示すように，食事中に含まれる鉄は上部消化管から吸収されて血液中に入り，血液中ではトランスフェリン（Tf）と結合して全身に運搬される．一部は肝臓で貯蔵されたり，筋肉などの全身の細胞で利用されるが，大部分の鉄はヘモグロビンの構成成分として骨髄での赤血球造血に利用される．産生された赤血球は全身を循環し酸素の運搬を行なうが，約120日の寿命を迎えると老廃赤血球は網内系にて破壊され，ヘモグロビンから取り出された鉄は再び血液中に入り再利用される．生体には鉄を積極的に排泄する機構が存在せず，消化管上皮細胞の脱落などによるわずかな鉄喪失しかない．一方で消化管から吸収される鉄も成人で約1 mg/日と少なく，ほとんどの鉄は再利用される鉄などで賄われており，半閉鎖的回路を構築している．

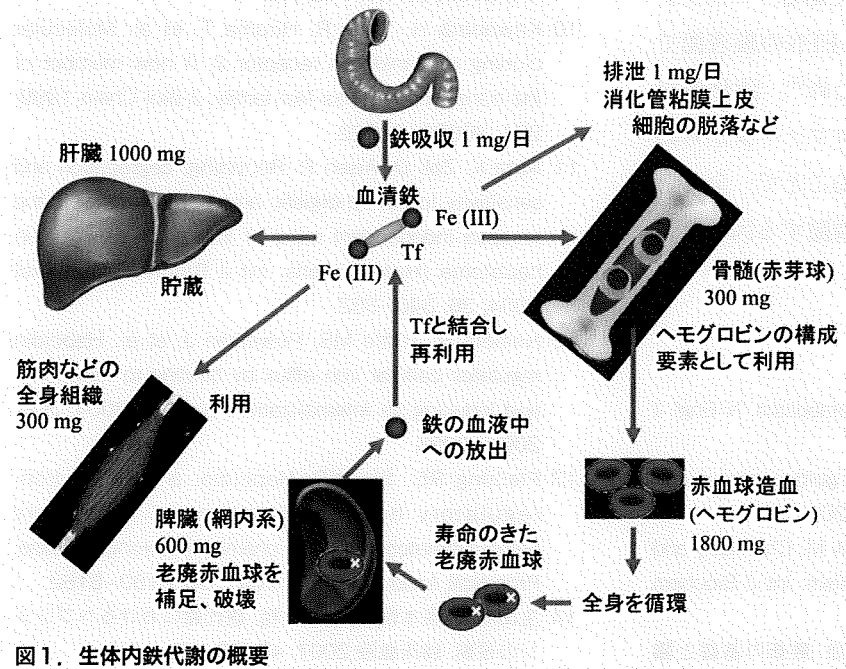

図1．生体内鉄代謝の概要

生体内鉄代謝の分子機構

このような生体内鉄動態であるが，近年の相次ぐ鉄代謝関連分子の同定に基づき分子機構についての理解が非常に進み，現在では**図2**のように理解されるようになっている[2-4]．

まず，鉄の吸収についてであるが，食事中に含まれる鉄はヘム鉄と非ヘム鉄に大きく分けられる．ヘム鉄の吸収に関しては残念ながら未だに詳細は解明されていないが，非ヘム鉄は，主に3価鉄の形であるが，上部小腸の腸管上皮細胞の腸管内腔側細胞膜上に存在するduodenal cytochrome b（Dcytb）によって2価に還元される[5]．2価鉄はdivalent metal transporter 1（DMT1）によって腸管細胞内に運ばれ[6]，その後，血管側に存在するフェロポーチン（FPN）によって血管内に放出される[7]．その際に2価鉄として放出される鉄をhephaestinが3価鉄に酸化している[8]．血液中に放出された3価鉄は通常1分子のトランスフェリンに対し2分子結合し，全身に運搬される．

骨髄中の赤芽球の膜表面には，トランスフェリンと高い親和性で特異的に結合するトランスフェリン・レセプター1（TfR1）が非常に多く発現しており，これによってトランスフェリン結合鉄は細胞内に取り込まれる．細

胞膜表面でトランスフェリンがTfR1と結合すると，エンドサイトーシスによって細胞内に入り，エンドソームからDMT1を介して鉄は細胞質に移動し，最終的にはミトコンドリアも関与してヘモグロビンの産生に利用される[9]．

網内系のマクロファージによる老廃赤血球の捕捉・破壊が起こると，得られた鉄はFPNを介して2価鉄として血液中に放出されるが，その際にはセルロプラスミン（CP）の持つ酸化作用によって3価に酸化され，再びトランスフェリンに結合して体内を循環し再利用されることになる．

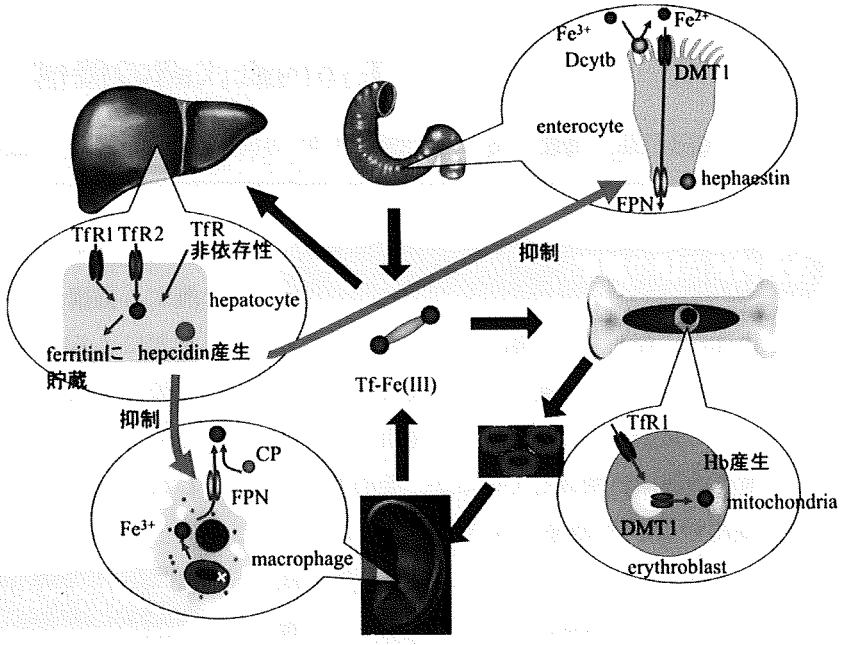

図2．生体内鉄代謝の分子機構

肝臓ではトランスフェリン結合鉄の一部が貯蔵されるが，肝細胞での鉄の取り込みにはTfR1やそのホモログ分子のトランスフェリン・レセプター2（TfR2）の関与が考えられているが[10]，これらの受容体に依存しない経路も想定されている[11]．

このように数多くの関連分子が関与して巧妙に制御され，なおかつ半閉鎖的な回路を構築している生体内鉄代謝であるが，これらを統合的に調節する因子がヘプシジンである．ヘプシジンは，主に肝臓で産生され血液中を循環する，活性型が25アミノ酸からなる小さなペプチドである．ヘプシジンは，腸管細胞や網内系におけるFPNの膜表面での発現を減少させるように働くため[12]，消化管での鉄吸収を抑制し，また，マクロファージからの鉄放出を抑制する方向に作用することで，全体として生体内鉄代謝を負の方向に調節する因子と判明している[2,4,13,14]．

文　献

1 Andrews NC. Disorders of iron metabolism. N Engl J Med 1999; 341: 1986–1995.
2 Andrews NC. Forging a field: the golden age of iron biology. Blood 2008; 112: 219–230.
3 Aisen P, Enns C, Wessling-Resnick M. Chemistry and biology of eukaryotic iron metabolism. Int J Biochem Cell Biol 2001; 33: 940–959.
4 生田克哉，鳥本悦宏，高後　裕.【貧血 最新の基礎と臨床】基礎編 貧血の分子病態 総論 鉄代謝と病態．日本臨牀 2008; 66: 469–474.
5 McKie AT, Barrow D, Latunde-Dada GO, et al. An iron-regulated ferric reductase associated with the absorption of dietary iron. Science 2001; 291: 1755–1759.
6 Gunshin H, Mackenzie B, Berger UV, et al. Cloning and characterization of a mammalian proton-coupled metal-ion transporter. Nature 1997; 388: 482–488.
7 Donovan A, Brownlie A, Zhou Y, et al. Positional cloning of zebrafish ferroportin1 identifies a conserved vertebrate iron exporter. Nature 2000; 403: 776–781.
8 Vulpe CD, Kuo YM, Murphy TL, et al. Hephaestin, a ceruloplasmin homologue implicated in intestinal iron transporter, is defective in the sla mouse. Nat Genet 1999; 21: 195–199.
9 Aisen P. Transferrin receptor 1. Int J Biochem Cell Biol 2004; 36: 2137–2143.
10 Kawabata H, Yang R, Hirama T, et al. Molecular cloning of transferrin receptor 2. A new member of the transferrin receptor-like family. J Biol Chem 1999; 274: 20826–20832.
11 Ikuta K, Zak O, Aisen P. Recycling, degradation and sensitivity to the synergistic anion of transferrin in the receptor-independent route of iron uptake by human hepatoma (HuH-7) cells. Int J Biochem Cell Biol 2004; 36: 340–352.
12 Nemeth E, Tuttle MS, Powelson J, et al. Hepcidin regulates cellular iron efflux by binding to ferroportin and inducing its internalization. Science 2004; 306: 2090–2093.
13 Fleming RE, Sly WS. Hepcidin: a putative iron-regulatory hormone relevant to hereditary hemochromatosis and the anemia of chronic disease. Proc Natl Acad Sci U S A 2001; 98: 8160–8162.
14 生田克哉，鳥本悦宏，高後　裕．鉄代謝におけるヘプシジンの役割．臨床血液 2007; 48: 36–45.

補遺4 鉄代謝のバイオマーカー

生田克哉，高後　裕　旭川医科大学　内科学講座　消化器・血液腫瘍制御内科学分野

血清鉄

血液中において鉄は，分子量約８万のトランスフェリンと呼ばれる蛋白に結合した形で全身に運搬されているが，血清鉄は，トランスフェリンに結合した鉄量を示している．

血清鉄は，鉄欠乏や鉄過剰といった生体内の鉄の状態変化の有無を確認するために，最も広く検査される項目である．血清鉄の正常値は施設によって異なるものの概ね70～160 μg/dlであるが，その解釈には注意が必要である．鉄は消化管から吸収され，血液中に入ってトランスフェリンと結合して運搬され，骨髄中の赤芽球をはじめとした全身の細胞に取り込まれて利用され，寿命を迎えた赤血球が網内系マクロファージで破壊されて鉄が再び放出され再利用されるといった一連の動きを呈しており，血清鉄は，採血時におけるそうした鉄の動的平衡状態を示している．そのため，ある一点での検査で全身の鉄代謝の状態を全て反映しているわけではない．例えば，血清鉄は，食後には消化管から流入した鉄がトランスフェリンと結合するために増加するし，鉄剤を服用後には増加することが知られているため，留意が必要である．血清鉄は，生体内鉄代謝を調べる際に最も基本となる検査項目であることは間違いないが，少なくとも血清鉄のみではなく，他の関連指標と組み合わせて，鉄代謝状態の把握が必要である．

不飽和鉄結合能 unsaturated iron binding capacity (UIBC)と総鉄結合能total iron binding capacity (TIBC)

UIBCとは，まだ鉄と結合していないトランスフェリンと結合しうる鉄量を示したものである．これに対してTIBCとは，血液中に存在するすべてのトランスフェリンに結合しうる鉄量を示すものである．そのため，血清鉄を含めるとこれら三者の関係は，

血清鉄＋UIBC＝TIBC

として表わされる．

生体が鉄欠乏に傾くと，肝臓におけるトランスフェリンの合成が増加し，UIBCおよびTIBCは増加するため，生体内鉄代謝の状態を推測するのに非常に有用である．しかし，トランスフェリンが肝臓で合成されることから，例えば栄養状態が悪化した際や，肝硬変などで肝合成能が低下した際などにはそれを反映して低下があることがあり，結果の解釈に注意が必要な場合もある．

トランスフェリン飽和率

血液中の全トランスフェリンのうち，鉄を結合しているものの割合を示す指標であり，以下の式で表わされる．

トランスフェリン飽和率 (%) = [血清鉄 (μg/dl) /TIBC (μg/dl)] × 100

通常血液中では30%程度のトランスフェリンしか鉄で飽和されていないが，鉄過剰症などではこの値が上昇してくる．

血清フェリチン

フェリチンは，肝細胞をはじめとした各種細胞内に存在する分子量約45万の蛋白であり，H-サブユニットとL-サブユニットと呼ばれる２つの異なるサブユニットが計24個集合し，大きな殻状構造を形成し，その中に鉄を格納する機能を有する．フェリチンは，鉄が過剰に存在すると，それによる細胞障害を防ぐために発現が亢進するが，血液中でも検出され，その濃度は全身の鉄の貯蔵状態をよく反映するものと知られ，生体内鉄貯蔵を示すマーカーとして広く利用されている．

血清フェリチンが低下を示している際には，

生体は鉄欠乏状態にあると考えて問題ないが，増加している際には解釈に注意が必要な場合がある．血清フェリチンは，もちろん生体が鉄過剰に傾き，鉄貯蔵量が増加した際にも増加するが，鉄貯蔵量が変化しなくても炎症状態においては炎症性サイトカインの影響などを受け増加を呈することがある．

可溶性トランスフェリン・レセプター

トランスフェリン・レセプター1（TfR1）の細胞外ドメインが切断されて血液中に放出されたものであり，1986年に高後らによって初めて発見された[1, 2]．これは，骨髄赤芽球の全TfR1発現量とよく相関しており，骨髄赤芽球における細胞内鉄濃度，および骨髄における造血能を反映するとされている．貯蔵鉄量とは反比例する．

鉄欠乏性貧血と慢性疾患に伴う貧血との鑑別診断[3]，慢性疾患に伴う貧血に合併した鉄欠乏性貧血の診断[4, 5]とその治療のために極めて重要である．生体内鉄代謝マーカーとして有用であるが，我国では未だ測定が広く普及していないのが現状である．

ヘプシジン

ヘプシジンは，肝臓で産生されて血液中を循環し，消化管からの鉄吸収を抑制し，また，網内系マクロファージからの鉄放出も抑制することで，生体内鉄代謝を負の方向に傾ける鉄代謝調節因子である．ヘプシジンの活性型は25アミノ酸からなるため抗体の作製が困難とされ，その前駆体のプロヘプシジンを測定するキットは市販化されているが[6]，ヘプシジンそのものを測定できる信頼性・簡便性を備えた測定法が確立されていないのが現状である．血清ヘプシジンを測定できるようになると，各種の病態における鉄代謝の把握がさらに進むことになり，臨床の場での測定が広く可能になることが強く望まれる．

文　献

1 Kohgo Y, Nishisato T, Kondo H, et al. Circulating transferrin receptor in human serum. Br J Haematol 1986; 64: 277–281.
2 Kohgo Y, Niitsu Y, Kondo H, et al. Serum transferrin receptor as a new index of erythropoiesis. Blood 1987; 70: 1955–1958.
3 Ferguson BJ, Skikne BS, Simpson KN, Bayne RD, Cook JD. Serum transferrin receptor distinguishes the anemia of chronic disease from iron deficiency anemia. J Lab Din Med 1992; 119: 385–390.
4 Punnonen K, Irjala K, Rajamaki A. Serum trensferrin recertor and its ratio to serum ferritin in the diagnosis of iron deficiency. Blood 1997; 89: 1052–1057.
5 Rimon E, Levy S, Sapir A, Gelzer G, Peled R, Ergas D, Sthoeger ZM. Diagnosis of Iron deficiency anemia in the elderly by transferrin receptor-ferritin index. Arch Intern Med 2002; 162: 445–449.
6 Kulaksiz H, Gehrke SG, Janetzko A, et al. Pro-hepcidin: expression and cell specific localisation in the liver and its regulation in hereditary haemochromatosis, chronic renal insufficiency, and renal anaemia. Gut 2004; 53: 735–743.

Question Answer

Q-25　鉄欠乏・鉄欠乏性貧血の分類をどのように考え，鉄代謝のマーカーをどのように使用したら良いでしょうか？

A-25　鉄欠乏は生体貯蔵鉄が減少または枯渇した状態で，「貧血のない鉄欠乏」と「鉄欠乏性貧血」に大別されます．一般的に貯蔵鉄の指標として血清フェリチンの測定が有用で，その値が12 ng/ml以下では間違いなく鉄欠乏状態にあります．ただし，血清フェリチン値は，貯蔵鉄増加の他，炎症，腫瘍などの疾患でもその影響を受けて上昇することがあり，解釈にあたって注意が必要です．臨床的に鉄欠乏性貧血と診断するには，貧血であることと，鉄欠乏状態があることの2つを満足する必要があります．貯蔵鉄が枯渇すると，肝臓でのフェリチン合成の低下とそれと鏡像的にトランスフェリン合成の上昇（TIBCの上昇として表わされる）が生じるため，本学会指針の鉄欠乏の診断に関する記載で

は，貯蔵鉄低下（鉄欠乏）の指標として血清フェリチンとTIBCの増加が有用であることを述べています．血清鉄は血清中のトランスフェリンに結合した鉄の値を示し，その低下は，組織鉄欠乏ばかりでなく二次性貧血でも網内系細胞への鉄貯留によりその低下が生じることがあるため，貯蔵鉄低下の指標としての特異性は高くありません．トランスフェリン飽和率（TSATと表現されることがある）は，血清鉄値をTIBCで割った値で，赤血球前駆細胞への鉄の取り込みに直結していますので，低い場合には鉄欠乏性貧血を強く疑いますが，二次性貧血の可能性を除外する必要があります．腎性貧血ではトランスフェリン飽和率が20%以下で血清フェリチン値が100 ng/ml以下で，鉄欠乏状態と診断してよいとされていますが，この基準は二次性貧血の1つである腎性貧血患者を対象とした鉄剤使用における判断基準であり，本治療指針の鉄欠乏・鉄欠乏性貧血の診断基準とは別個の考え方で立てられていることをご承知ください．

Q-26　腎性貧血を扱う領域で機能性鉄欠乏（functional iron deficiency）やTSATなどの用語が使われていますが，これまでの血液学で鉄欠乏性貧血を扱う領域で使用する用語と違いがあるようですが，どう考えたら良いでしょうか？

A-26　腎性貧血では，エリスロポエチンなどの赤血球増加因子と鉄剤の併用が，ヘモグロビンの改善効果が強いことから，それらの現象を説明しエリスロポエチンと鉄剤使用の臨床的利便性のために，機能性鉄欠乏（functional iron deficiency）など新たな用語が使われていると理解しています．機能性鉄欠乏の用語は，二次性貧血とくに腎性貧血での鉄の利用障害，エリスロポエチン使用時の貯蔵鉄から骨髄赤血球造血への鉄の供給が不十分な際に生じる病態に対応し，腎性貧血治療時の反応を理解するのに便利であることから使用されていると考えられますが，一般の鉄代謝における「貯蔵鉄が枯渇している鉄欠乏」とは別の概念として捉えておくことが良いでしょう．また，「機能性」鉄欠乏に対して，「絶対的」鉄欠乏という用語が使われることもありますが，鉄欠乏の定義自体が，生体貯蔵鉄が欠乏している状態をすでにさしているため，あえて「絶対的」という言葉を使用する必要はないでしょう．現在，ヘプシジンをはじめ二次性貧血に伴う鉄代謝異常の病因・病態究明が急速に進んでいますので，鉄欠乏，貯蔵鉄の利用障害を生じさせている病態を理解・整理しながら用語を使われるのが良いでしょう．

doi:10.1016/j.jmb.2010.01.026 J. Mol. Biol. (2010) 397, 375–384

JMB

Available online at www.sciencedirect.com

ScienceDirect

ELSEVIER

Characterization of the Interaction between Diferric Transferrin and Transferrin Receptor 2 by Functional Assays and Atomic Force Microscopy

Katsuya Ikuta[1,2]*, Alexandre Yersin[3], Atsushi Ikai[3], Philip Aisen[2] and Yutaka Kohgo[1]

[1]*Division of Gastroenterology and Hematology/Oncology, Department of Medicine, Asahikawa Medical College, 2-1-1-1 Midorigaoka-Higashi, Asahikawa, Hokkaido 078-8510, Japan*

[2]*Department of Physiology and Biophysics, Albert Einstein College of Medicine, 1300 Morris Park Avenue, Bronx, NY 10461, USA*

[3]*Graduate School of Bioscience and Biotechnology, Tokyo Institute of Technology, 4259-B8 Nagatsuta-cho, Midori-ku, Yokohama 226-8501, Japan*

Received 11 August 2009; received in revised form 29 December 2009; accepted 13 January 2010
Available online 22 January 2010

Edited by W. Baumeister

Transferrin receptor 2 (TfR2), a homologue of the classical transferrin receptor 1 (TfR1), is found in two isoforms, α and β. Like TfR1, TfR2α is a type II membrane protein, but the β form lacks transmembrane portions and therefore is likely to be an intracellular protein. To investigate the functional properties of TfR2α, we expressed the protein with FLAG tagging in transferrin-receptor-deficient Chinese hamster ovary cells. The association constant for the binding of diferric transferrin (Tf) to TfR2α is $5.6\times10^6\ M^{-1}$, which is about 50 times lower than that for the binding of Tf to TfR1, with correspondingly reduced rates of iron uptake. Evidence for Tf internalization and recycling via TfR2α without degradation, as in the TfR1 pathway, was also found. The interaction of TfR2α with Tf was further investigated using atomic force microscopy, a powerful tool used for investigating the interaction between a ligand and its receptor at the single-molecule level on the living cell surface. Dynamic force microscopy reveals a difference in the interactions of Tf with TfR2α and TfR1, with Tf–TfR1 unbinding characterized by two energy barriers, while only one is present for Tf–TfR2. We speculate that this difference may reflect Tf binding to TfR2α by a single lobe, whereas two lobes of Tf participate in binding to TfR1. The difference in the binding properties of Tf to TfR1 and TfR2α may help account for the different physiological roles of the two receptors.

Keywords: iron metabolism; transferrin; transferrin receptor 2; atomic force microscopy; functional assay

Introduction

Iron is essential for all living organisms and is required for numerous metabolic processes. In vertebrates, and at least in some invertebrates with circulatory systems, almost all circulating iron is carried by diferric transferrin (Tf) to provide iron for cellular needs. The initial event in the cellular uptake of iron is the binding of Tf to transferrin receptor 1 (TfR1)[1] on the plasma membrane of cells, followed by endocytosis of the Tf–TfR1 complex. HFE[2]—the protein that, when mutated, is responsible for hereditary hemochromatosis—has been shown to combine with TfR1

*Corresponding author. 2-1-1-1 Midorigaoka-Higashi, Asahikawa, Hokkaido 078-8510, Japan. E-mail address: ikuta@asahikawa-med.ac.jp.

Present addresses: A. Yersin, Gymnase de Beaulieu, Rue du Maupas 50, 1004 Lausanne, Switzerland; A. Ikai, Innovation Laboratory, Tokyo Institute of Technology (S2-8), 4259, Nagatsuta-Cho, Midori-Ku, Osaka, Japan.

Abbreviations used: TfR2, transferrin receptor 2; TfR1, transferrin receptor 1; Tf, diferric transferrin; AFM, atomic force microscopy; CHO, Chinese hamster ovary; PBS, phosphate-buffered saline; TCA, trichloroacetic acid; PTA, phosphotungstic acid; GFP, green fluorescent protein; BSA, bovine serum albumin.

0022-2836/$ - see front matter

and to reduce its affinity for Tf,[3–6] but the physiological functions of HFE are still not fully understood. In the acidified Tf-bearing endosome, iron is released from Tf and carried into the cytosol by divalent metal transporter 1.[7–9] After the release of its iron, Tf, still bound to the receptor in the acidified endosome, is recycled to the cell membrane and released from TfR1 at the cell surface where iron-free Tf is not bound by the receptor at pH 7.4. Most cells other than hepatocytes have been thought to depend chiefly or exclusively on the TfR1 cycle for securing iron from Tf.[10–12]

A second transferrin receptor, transferrin receptor 2 (TfR2), was cloned and identified as a new member of the transferrin receptor class.[13] TfR2 has two isoforms: TfR2α and TfR2β. TfR2α is thought to be a type II membrane protein like classical TfR1.[14] TfR2β is probably an intracellular protein because its amino acid sequence lacks transmembrane portions. Although its affinity for Tf is less than that for TfR1, TfR2α binds Tf and therefore may participate in cellular iron uptake, while the physiological function of TfR2β is unknown. Mutations of the TfR2 gene reduce hepcidin expression, resulting in iron overload and indicating that TfR2 may function primarily as a regulator of hepcidin production. However, the precise mechanisms of TfR2α involvement in cellular iron metabolism have not been elucidated, largely due to lack of information about the properties of the TfR2α protein. We therefore aimed to characterize the interactions of TfR2α with Tf by functional assays and atomic force microscopy (AFM), a powerful tool for investigating the interaction between a ligand and its receptor at the single-molecule level on a living cell surface.[15]

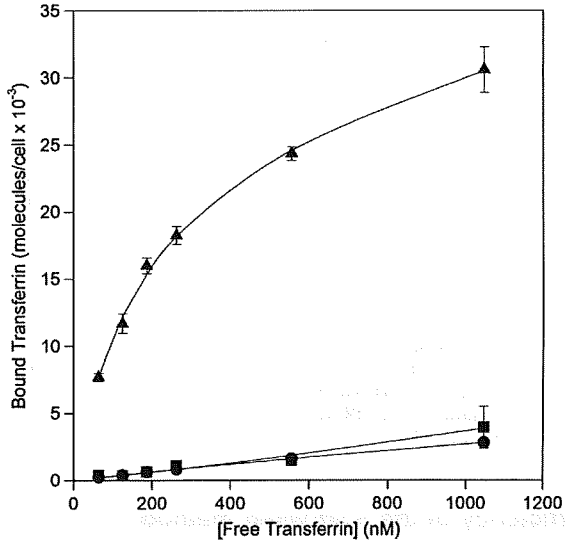

Fig. 1. Tf binding to TRVb (●), TRVb-TfR2α (▲), and TRVb mock cells (■) at 4 °C. Cells were incubated with [^{125}I]Tf at 4 °C for 1 h, washed to remove unbound Tf, and then solubilized for counting. TRVb-TfR2α cells showed a saturable binding curve, with an association constant of 5.6×10^6 M^{-1} and 2.8×10^4 binding sites/cell. The experiment was performed in triplicate.

Results

Total protein contents

TfR1-deficient Chinese hamster ovary (CHO) TRVb cells were transfected with a TfR2α expression vector or mock vector, with no detectable change in cell morphology observed in culture wells by light microscopy. The total protein contents were 113± 20 pg/cell ($n=10$) for wild-type TRVb cells, 127± 19 pg/cell ($n=10$) for TRVb-TfR2α cells, and 120± 15 pg/cell ($n=10$) for TRVb mock cells. Thus, transfection of TRVb cells with the TfR2α expression vector did not cause any remarkable change in cellular protein concentration.

Expression of TfR2α and its binding to Tf

Transfection of TRVb cells with the TfR2α expression vector resulted in much higher Tf binding at 4 °C compared to wild-type TRVb cells or the mock-transfected clone (Fig. 1). Tf binding to TRVb cells and TRVb mock cells showed a nonsaturable, almost linear, behavior characteristic of nonspecific binding. In contrast, expressed cell surface Tf binding sites in TRVb-TfR2α cells saturated at 2.8×10^4 Tf molecules/cell, with the association constant K_a calculated to be 5.6×10^6 M^{-1}. Since TRVb-TfR2α cells and TRVb mock cells were maintained at 30 μg/ml puromycin, but TRVb cells were maintained without puromycin, TRVb mock cells were used as controls for further studies.

Cell-associated Tf at 37 °C

Total cell-associated Tf at 37 °C increased as a function of Tf concentration in TRVb-TfR2α cells (Supplementary Fig. 1). The cell-associated Tf of TRVb mock cells, however, also increased as a function of Tf concentration, even though cell-associated Tf was less than that seen in TRVb-TfR2α cells. To determine whether transfection was responsible for this increase in cell-associated Tf in mock cells, we measured cell-associated Tf in wild-type TRVb cells at 37 °C. There was no remarkable difference between wild-type TRVb and TRVb mock cells, indicating that transfection itself did not cause the Tf association in mock cells (data not shown). Since TRVb cells lack detectable TfR1, this association with Tf must be receptor-independent. The difference between cell-associated Tf in TRVb-TfR2α cells and cell-associated Tf in TRVb mock cells as a function of Tf concentration—presumably due to Tf bound to TfR2α and Tf internalized via TfR2α in the former, but not in the latter—approached a constant value.

Table 1. Tf internalized by TRVb-TfR2α cells via TfR2α

Procedure	Molecules/cell
[1] Total Tf associated with TRVb-TfR2α cells after incubation for 1 h at 37 °C	47,800
[2] Cell-associated Tf after acid washing	26,500
[3] Tf removed by acid washing	21,300
[4] Tf initially bound to TfR2α at the cell surface (10/9×[3])	23,700
[5] Tf initially bound to TfR2α at the cell surface but resistant to acid washing	2370
[6] Tf internalized by all pathways ([2]–[5]), also non-specifically bound and resistant to acid washing	24,100
[7] Tf in mock cells (non-specifically bound and resistant to acid wash)	6600
[8] Tf internalized via TfR2α in TRVb-TfR2α cells ([6] and [7])	17,500

Efficiency of the acid wash method

Our acid wash method removed approximately 90% of the cell surface membrane-bound Tf in TRVb-TfR2α cells compared to normal phosphate-buffered saline (PBS) washing (data not shown). In addition to acid washing, washing with F-12 medium was necessary to remove bound Tf, suggesting that, like TfR1, TfR2α binds apotransferrin at acidic pH but not at neutral pH.[14] Addition of cold Tf into F-12 medium at pH 7.4 did not enhance the effectiveness of washing, verifying that washing at pH 7.4 is sufficient for removing cell-surface-bound apotransferrin.

Evidence for Tf internalization mediated by TfR2α

After 1 h of incubation at 37 °C, cell-associated Tf in TRVb-TfR2α cells and TRVb mock cells represents both internalized Tf and nonspecific cell-surface-bound Tf that are resistant to acid washing. Tf in TRVb-TfR2α cells was 26,500 molecules/cell, much higher than the 6600 molecules/cell seen in TRVb mock cells (Table 1). Although the effectiveness of the acid wash method is only about 90%, the difference in cell-associated Tf between transfected cells and mock cells is too great to be attributed to residual cell-surface-bound Tf and therefore represents Tf internalized via TfR2α. We calculate that about 17,500 Tf molecules/cell are internalized by TfR2α (Table 1).

Iron uptake

Iron uptake by TRVb-TfR2α cells after 1 h of incubation at 37 °C was not clearly different from that by TRVb mock cells, even though there were small differences at high concentrations of Tf (Fig. 2a). To investigate whether or not induced TfR2α protein actually can donate iron to the cells, we determined the time course of ^{59}Fe uptake. Only after 1 h did a difference between TRVb-TfR2α cells and TRVb mock cells become clear (Fig. 2b). Thus, TfR2α-associated Tf could donate iron to cells, although its rate of donation is much less than that provided by Tf associated with TfR1. The data also indicate that CHO cells exhibit receptor-independent iron uptake from Tf, as described earlier.[16]

Efflux of Tf

To investigate the fate of Tf taken up through TfR2α, we incubated TRVb-TfR2α cells with ^{125}I-labeled Tf and acid-washed them before the time course of efflux was determined (Fig. 3). At time 0, Tf internalization by TRVb-TfR2α cells was higher than

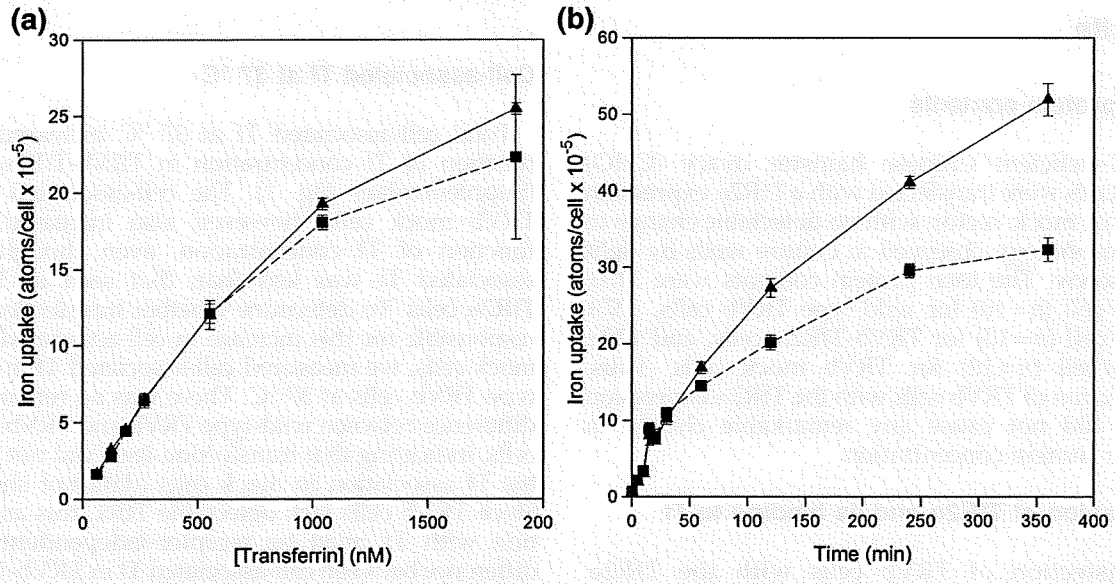

Fig. 2. Iron uptake at 37 °C as a function of Tf concentration (a). TRVb-TfR2α cells (▲) and TRVb mock cells (■) were incubated with [^{59}Fe]Tf at 37 °C for 1 h, washed to remove unbound Tf, and then solubilized for counting. This experiment was performed in triplicate. Iron uptake at 37 °C with time was also investigated (b). TRVb-TfR2α cells (▲) and TRVb mock cells (■) were incubated with 8.1×10^{-7} M [^{59}Fe]Tf at 37 °C for the indicated time, washed to remove unbound Tf, and then solubilized for counting. This experiment was also performed in triplicate.

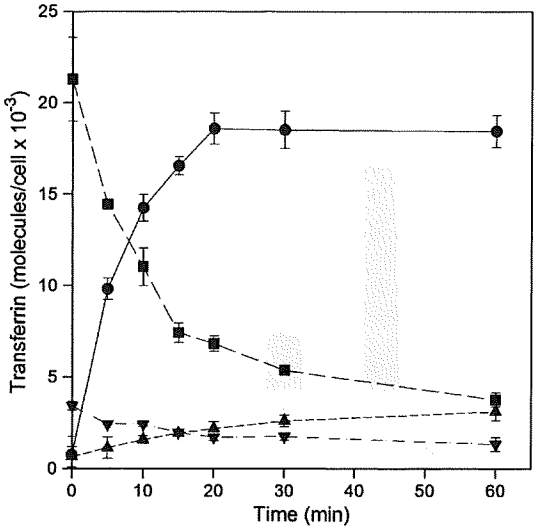

Fig. 3. Time course of Tf efflux. TRVb-TfR2α cells and TRVb mock cells were incubated with 3.5×10^{-7} M [^{125}I]Tf at 37 °C for 1 h, washed to remove unbound Tf, and then acid-washed to remove Tf bound to cell surface receptors. Cells were then incubated at 37 °C for the indicated times, the medium was collected, and solubilized cells were taken for counting. Tf exocytosed into the medium from TRVb-TfR2α cells (●) and TRVb mock cells (▲), and Tf retained in TRVb-TfR2α cells (■) and TRVb mock cells (▼), are shown. Experiments were performed in triplicate.

Tf internalization by TRVb mock cells, in keeping with Tf internalization by TfR2α, as discussed above. Internalized Tf mediated by TfR2α was exocytosed from TRVb-TfR2α cells; approximately 80% of Tf taken up via TfR2α was released by 30 min. The indication is that an effective efflux route exists for Tf taken up by TfR2α, suggesting that TfR2α, like TfR1, is recycled by the cells.

In a further investigation of the TfR2α pathway, the degradation of Tf internalized by TfR2α was determined. After 60 min, approximately 90% of Tf exocytosed from TRVb-TfR2α cells was precipitable by trichloroacetic acid (TCA)/phosphotungstic acid (PTA), indicating that Tf bound to TfR2α has recycled without substantial degradation in cells.

Pulse-chase study

To determine the fraction of cell-membrane-bound Tf that is internalized and the recycling time, we performed a pulse-chase experiment (Supplementary Fig. 2). Almost all Tf initially bound to TfR2α at 4 °C was released into the culture medium after 10 min of incubation at 37 °C, and there was no significant internalization of cell-surface-bound Tf in the single cycle of this pulse-chase study.

Absence of TfR1–TfR2 heterodimers

The effectiveness of anti-FLAG M2 antibody and anti-TfR1 antibody in immunoprecipitation had been confirmed before these experiments were undertaken (data not shown). HuH-7 cells, which express detectable TfR1 by Western blot analysis, were transiently transfected with the TfR2α expression vector, and cell lysates were taken for immunoprecipitation and Western blot analysis (Supplementary Fig. 3). Western blot analysis by anti-TfR1 antibody for the samples without immunoprecipitation showed that HuH-7 cells and HuH-7 cells transfected with TfR2α express almost identical amounts of TfR1. Furthermore, Western blot analysis by anti-TfR2 antibody for the samples not subjected to immunoprecipitation showed that HuH-7 cells transfected with TfR2α express more TfR2α proteins than nontransfected HuH-7 cells. These data indicated that the transiently transfected cells overexpressed TfR2α protein and that the antibodies were highly effective for Western blot analysis. When immunoprecipitation was performed with anti-TfR1 antibody, a band was clearly detected in transfected and nontransfected cells, but no band was found with the anti-TfR2 antibody. If a TfR1–TfR2 heterodimer were present, anti-TfR1 antibody would precipitate that protein, and Western blot analysis with anti-TfR2 antibody would show the band. When immunoprecipitation was performed with anti-FLAG M2 antibody, a 100-kDa band was detected only in transfected cells when the anti-TfR2 antibody was used as the primary antibody in Western blot analysis, indicating that transient transfection resulted in expression of immunoprecipitable TfR2α protein. No band was detected when anti-TfR1 was used as the primary antibody. Prolonged exposure of the blotted membrane to the developing solution did not make a difference. The possibility that the N-terminal FLAG tag in TfR2α interferes with dimer formation is unlikely, since the recombinant TfR1 lacking the first 120 N-terminal intracellular residues spontaneously dimerizes.[17] These results indicate that no detectable heterodimer of TfR1 and TfR2α was formed by the TfR2α-transfected HuH-7 cells. Therefore, our experiments detect TfR2, not the heterodimer of TfR1 and TfR2.

Specificity of detection by AFM

HLF cells (human hepatoma) were transiently cotransfected with TfR2α and green fluorescent protein (GFP) for identification, and tested with a Tf-coated tip. Retraction force curves were recorded with a Tf-coated tip and showed specific unbinding events between Tf on the tip and TfR2α at the cell surface (in Tris-buffered saline, pH 7.4) (Fig. 4a). The probability of binding between the Tf-coated tip and the TfR2 at the cell surface reached 26% ($n=7$ cells). In contrast, when nontransfected cells were tested with a Tf-coated tip, this probability was only 6% ($n=12$ cells, $p<0.001$, t test). This indicated that transient transfection of the TfR2α expression vector was adequate for the investigation using AFM (Fig. 4b).

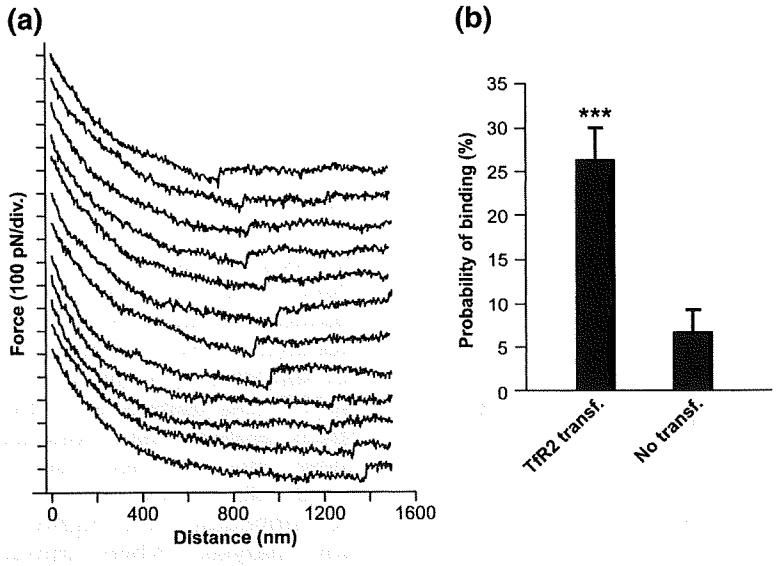

Fig. 4. (a) Retraction force curves on living HLF cells, transfected with TfR2α. The curves show specific unbinding events between Tf on the probe tip and TfR2α at the cell surface [in Tris-buffered saline (pH 7.4)]. (b) Specificity of detection by AFM. HLF cells (human hepatoma) were transiently cotransfected with TfR2α and GFP, and tested with a Tf-coated tip. The probability of binding was 26% ($n=7$ cells). In contrast, on nontransfected cells, the probability was only 6% ($n=12$ cells, $p<0.001$,***t test).

Force histogram for specific interaction between Tf and TfR2α

We recorded 1500 force curves with a Tf-coated tip on TfR2-transfected cells, allowing us to collect a total of 573 specific unbinding events in an experiment performed with a single tip using two cells. Events were analyzed and plotted in a force histogram (Fig. 5). A clear peak was visible on the histogram, showing that the mean unbinding force between Tf on the tip and TfR2 at the cell surface was 63±8 pN (at a mean loading rate of 2.8 nN/s). The experiment was repeated several days later using a new tip with cells independently cultured and gave similar results.

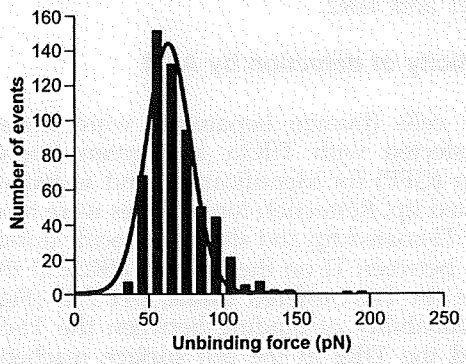

Fig. 5. Force histogram for the specific interaction between Tf and TfR2α on HLF cells. The histogram was obtained from an analysis of 573 unbinding events collected over 1500 force curves. The mean unbinding force is 63±8 pN for a mean loading rate of 2.8 nN/s. The gray line represents a Gaussian fit.

Dynamic force spectroscopy

Dynamic force spectroscopy, which consists of measuring the mean unbinding force at different loading rates, was performed with a Tf-coated tip on TfR2-transfected cells. As expected, the force was logarithmically dependent on the loading rate (Fig. 6). However, this dependence was small, as the force varied from 59±9 pN at a rate of 1.7 nN/s to 62±10 pN at a rate of 20 nN/s. In striking contrast, the unbinding force between TfR1 and Tf was reported at 39±5 pN at a rate of 1 nN/s and

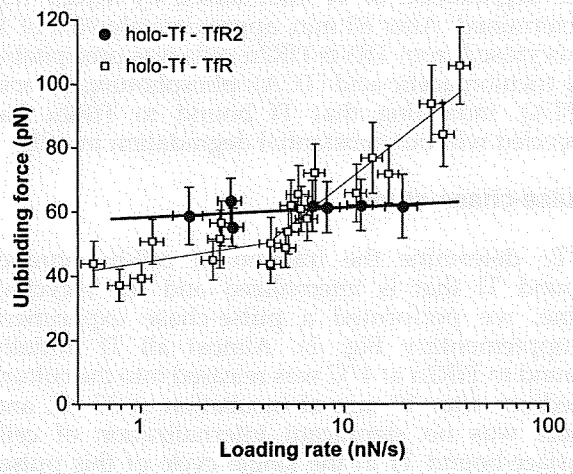

Fig. 6. Dynamic force spectroscopy of Tf–TfR2α (black dots). The unbinding force is plotted as a function of the loading rate logarithm. For comparison, the force spectrum of Tf–TfR1 is also shown. Only one regime is evident for TfR2, but two can be seen for TfR1, clearly revealing the different interactions of the two proteins with Tf.

increased up to 94±12 pN at a rate of 27 nN/s,[15] indicating that the binding of TfR2α and Tf differs from the binding of TfR1 and Tf. Furthermore, the force spectrum of TfR2-transfected cells displayed only one regime (slope), while two regimes were clearly visible for TfR1-expressing cells (Fig. 6), implying different interactions of Tf with TfR1 and TfR2.

Discussion

In their original publication, Kawabata *et al.* reported that TfR2α can bind Tf and donate iron to CHO cells,[13] therefore supporting cell growth.[14] Fleming *et al.* found that TfR2 expression is not regulated by intracellular iron status and thus might be involved in the pathogenesis of hemochromatosis.[18] Although TfR2 is thus shown to function in iron metabolism, its precise physiological role is still unknown.

To avoid confusion by TfR1, our first studies used HuH-7 cells with anti-sense suppressed TfR1 expression.[19,20] The amount of residual TfR1, however, was still high, so that it was not possible to differentiate between Tf binding to TfR1 and Tf binding to TfR2α because of the low affinity of TfR2α for Tf.[14] We therefore turned to TfR1-deficient CHO cells for expressing TfR2α.[13,21]

In the present study, the affinity of TfR2α for Tf was measured in living cells for the first time using [^{125}I]Tf to display the binding isotherm at 4 °C. The K_a for the binding of Tf by TfR2α was calculated to be 5.6×10^6 M^{-1}, about 35-fold less than that for the binding of Tf by TfR1 (2×10^8 M^{-1} to 3×10^8 M^{-1} in HuH-7 cells). The lower affinity of TfR2α in transfected CHO cells is in accordance with a previous report based on a qualitative study by flow cytometry.[14] Quantification by surface plasmon resonance using a recombinant soluble extracellular portion of the receptor gave a binding constant of 37×10^6 M^{-1}, consistent with the present result, considering the difference in methodology.[22] The deduced amino acid sequence of the extracellular domain of TfR2α protein is 45% identical and 66% similar to that of TfR1. TfR2α also possesses the RGD triad (amino acids 678–680),[13] which is thought to be critical for binding Tf to TfR1.[23] The lower affinity of TfR2α for Tf is now, therefore, not explicable.

Although the affinity of TfR2α for Tf is much less than that of TfR1, the concentration of iron-bearing Tf in the circulation (about 3×10^{-5} M) is sufficient to saturate TfR2α. TfR2α expression has been found in cells with active roles in iron metabolism. Liver, the principal organ of iron storage, expresses a high level of TfR2α mRNA, as do human hepatoma-derived HepG2 cells[13] and HuH-7 cells (unpublished observation). K562 cells, of human myelogenous erythroleukemic origin, also express TfR2α mRNA.[13] Studies of iron uptake from Tf prior to the discovery of TfR2 did not discriminate between the roles of the two receptors. In future studies, therefore, both receptors require consideration.

Binding of Tf to TRVb-TfR2α and TRVb mock cells at 4 °C was only 25–50% inhibited by a 100-fold excess of unlabeled Tf, possibly because of large, essentially nonsaturable binding. We therefore resorted to the use of a binding isotherm with terms for specific (saturable) and nonspecific (nonsaturable) binding to estimate the binding constants for each type of binding.[24] Curve-fitted parameters for specific binding attributable to transfected TfR2α were as follows: K_a, 5.6×10^6 M^{-1}; total number of sites, 2.8×10^4 $cell^{-1}$. These contrast with binding constants near 10^8 M^{-1} and site numbers in the range of 2×10^5 $cell^{-1}$ to 5×10^5 $cell^{-1}$ for Tf binding in K562 cells when TfR1 predominates and curve-fitting to a single class of sites adequately accounts for binding. An apparent binding constant of 6.5×10^9 M^{-1} is obtained for the nonsaturable binding of Tf to TRVb-TfR2α cells, substantially weaker than that derived for specific binding. At Tf concentrations of 10^{-6} M, for example, saturable binding would account for about 24,000 Tf molecules/cell, while nonsaturable binding would account for 6500 molecules/cell. Nevertheless, both TfR2α-dependent binding and nonspecific binding contribute to the association of Tf with the cells.

In the present study, CHO cells showed a receptor-independent association with Tf that should be considered when investigating the function of TfR2α expressed in CHO cells. We find a clear increase in cell-associated Tf after TfR2α expression. Since cell-associated Tf represents both cell-surface-bound Tf and Tf internalized via TfR2α, a proof of Tf internalization mediated by TfR2α was required. Cell-associated Tf persisting after acid washing confirmed the existence of Tf internalization via TfR2α.

After internalization, an efflux of Tf, without substantial degradation, is found. Thus, Tf internalized by TfR2α, like Tf internalized by TfR1, recycles. An important difference between the two receptors was observed in a pulse-chase study. Less than 12% of Tf bound to the cell surface of TRVb-TfR2α cells is internalized, with most of the Tf dissociated and released to the medium at 37 °C. In contrast, approximately 30–50% of membrane-bound Tf was internalized by human-hepatoblastoma-derived HepG2 cells[12] and human-hepatoma-derived HLF cells.[25] The lower affinity of TfR2α for Tf may help account for the difference between previous studies and the present work, since HepG2 and HLF cells express TfR1, but TRVb-TfR2α cells do not. In our pulse-chase study, no detectable internalization of membrane-bound Tf in a single cycle was found when the occupancy of TfR2α by transferrin was about 75%. In normal circulation, however, the concentration of iron-bearing Tf is close to 3×10^{-5} M, so that cell surface receptors are always saturated with Tf and replenished as Tf is internalized. TfR2α might therefore normally function in iron uptake from Tf, but this has yet to be experimentally confirmed.

Overexpressed TfR2α protein was also shown to mediate iron uptake, although its rate of iron donation was slow. We estimate, from the difference between iron uptake by TRVb-TfR2α cells and iron uptake by TRVb mock cells in Fig. 2b, that the rate of iron uptake was approximately 0.2 atom/receptor/min when cells were incubated with 8.1×10^{-7} M Tf. For comparison, the rate of iron uptake via TfR1 was about 0.5–1 atom/receptor/min in K562 cells. Thus, TfR2α may function in iron uptake from Tf, albeit with less efficiency than TfR1.

Because of the sequence similarities between TfR1 and TfR2α, the possibility that the protein monomers combine to form heterodimers was investigated. However, no detectable expression of heterodimers was found in the present studies. The possibility that our transfection procedure in HuH-7 cells yielded two different cell populations (one expressing TfR2α and the other failing to do so) must be considered, so that expression of heterodimers was too low for detection. We cannot exclude the possibility of heterodimer formation that might be detected by more sensitive methods or in other cells.

AFM was used to characterize the interactions between Tf and TfR2α protein at the single-molecule level. We found that the unbinding force needed to detach Tf from TfR2α (63±8 pN) was different from the unbinding force needed to detach Tf from TfR1, previously reported as 56±7 pN.[15] However, dynamic force measurements revealed striking differences between Tf–TfR1 and Tf–TfR2α interactions, which reflected clearly distinct energy landscapes.[15] While Tf–TfR1 unbinding is characterized by two energy barriers, only one is present for Tf–TfR2. This obvious difference might arise from different binding points for Tf–TfR1 and Tf–TfR2α interactions. In addition, this possibility provides a structural interpretation for the energy barriers postulated here. We speculate that the two barriers of the Tf–TfR1 interaction stem from the binding of both lobes of Tf (C-lobe and N-lobe), whereas the single barrier of Tf–TfR2α interaction originates from the binding of a single lobe, but we recognize that this speculation requires further investigation.

In conclusion, the present study shows that TfR2α protein functions in binding Tf and taking up iron, and that there must be a difference between TfR1 and TfR2 in their interactions with Tf, as revealed by AFM. TfR2α mRNA lacks an iron responsive element, so that expression is not regulated by intracellular iron status[18] but possibly by cell cycle.[14] Furthermore, TfR2 cannot compensate for TfR1 in TfR1 knockout mice, which lack a functional Tf cycle and do not survive gestation.[26] A nonsense mutation of the human TfR2 gene causes a hemochromatosis-like disorder.[27,28] The physiological functions of TfR2 are therefore still unclear, although it likely contributes to the regulation of cellular iron status.

Materials and Methods

Cells and cell culture

TfR1-deficient CHO TRVb cells[21] were grown in F-12 Nutrients Mixture (Invitrogen, Grand Island, NY) supplemented with 5% heat-inactivated fetal bovine serum (Gemini Bio-Products, Woodland, CA), 100 U/ml penicillin, and 100 μg/ml streptomycin. All cultures were maintained at 37 °C in 5% CO_2.

TfR2α expression vector

Total RNA was extracted from K562 cells using the RNAgent Total RNA Isolation System (Promega, Madison, WI) following the manufacturer's instructions. Complementary DNA was reverse-transcribed from 1 μg of RNA using an oligo-dT primer (Promega) and MMLV reverse transcriptase (Stratagene, La Jolla, CA), and human TfR2α cDNA was amplified by hot-start PCR. A FLAG sequence was added to the 5′-terminus of the cDNA to enable detection of expressed protein by anti-FLAG antibodies. The oligonucleotides used as PCR primers were 5′-ACCTTAAGGCCACCATGGATTACAAGGATGACGACGATAAGATGGAGCGGCTTTG-3′ and 5′-GGTTCGAAGCAATGAGAGGTGGAC-3′. The conditions for amplification were as follows: 40 cycles of 99 °C for 1 min, 65 °C for 2 min, and 72 °C for 5 min. The amplified DNA fragment was digested with AflII and BstBI, and then inserted into the bicistronic mammalian expression vector pIRESpuro2 (Clontech, Palo Alto, CA). The orientation and sequence of the inserted TfR2α cDNA fragment were confirmed by sequencing.

Transfection

TRVb cells were grown in 35-mm six-well plates until they had reached 70–80% confluence, then they were transfected with the TfR2α expression vector using Lipofectamine Plus (Invitrogen, Carlsbad, CA). Selection was performed with 10 μg/ml puromycin (Clontech) for 2 weeks, and then the concentration of the antibiotic was raised to 30 μg/ml in order to isolate a clone with high-level expression of TfR2α. After another 2 weeks, one viable colony (TRVb-TfR2α) was obtained and then subcultured using a cloning cylinder. As mock-transfected controls, TRVb cells were transfected with the pIRESpuro2 vector without a cDNA insert, and one clone was isolated after 4 weeks of selection (TRVb mock cells). These transfectants were maintained at 30 μg/ml puromycin after isolation. Expression of TfR2α mRNA was confirmed by reverse transcriptase PCR, and the expression of TfR2α protein was confirmed by immunoprecipitation–Western blot analysis using anti-FLAG antibodies (data not shown).

Total protein content

The total protein contents of TRVb, TRVb-TfR2α, and TRVb mock cells were determined with the Bio-Rad Protein Assay Kit (Bio-Rad, Hercules, CA) using bovine serum albumin (BSA) as standard. Cells were counted with a hemocytometer.

Iodination of Tf

Human Tf (Boehringer-Mannheim, Germany) was labeled with ^{125}I (Amersham Pharmacia Biotech, Piscataway, NJ) by the iodine monochloride method of McFarlane.[29] To remove unbound ^{125}I, we passed labeled Tf through a 10-DG desalting column (Bio-Rad) two times. Specific activities were observed in the range of 100–200 cpm/ng Tf, and more than 95% of ^{125}I was protein-bound as determined by precipitation with 20% TCA/4% PTA.

^{59}Fe labeling of Tf

Iron was removed from Tf, and labeling with ^{59}Fe was carried out by previously described methods.[30] Specific activities were in the range of 2000–3500 cpm/ng Fe. In some experiments, apotransferrin was labeled with ^{125}I, as described above, and then loaded with ^{59}Fe.

Binding assay

Tf binding assays were performed as previously reported.[31] Cell numbers were calculated from protein concentrations determined with the Bio-Rad Protein Assay Kit. Each experiment was performed in triplicate. The total number of specific binding sites per cell and the K_a for the binding of Tf to these sites were estimated from nonlinear least-squares curve fitting to a saturable binding isotherm:[32]

$$\text{occupied sites} = \frac{\text{total sites} \times K_a[\text{Tf}]}{1 + K_a[Tf]}$$

from which it is also possible to calculate the fraction of sites occupied by Tf at any concentration of free Tf.

Tf and iron uptake

Cells were plated at a density of 1×10^6 cells/well in 35-mm six-well plates 24 h before the experiments. Cells were preincubated with F-12 three times for 10 min at 37 °C, chilled on ice for 30 min, and then incubated at 37 °C with F-12 containing 2% BSA and labeled Tf at indicated concentrations and times. Cells were then washed with ice-cold PBS five times and solubilized by 0.1% Triton X-100 for counting.

Acid washing of cells

To remove cell-surface-receptor-bound Tf, we washed cells with ice-cold PBS five times and then incubated them with ice-cold acid wash buffer [0.025 M citric acid, 0.025 M sodium citrate, 200 μM deferoxamine mesylate, and 0.15 M sucrose (pH 4.0)] for 3 min, followed by two 2-min incubations with ice-cold F-12 medium to remove cell-surface-bound apotransferrin. Finally, the cells were washed once more with ice-cold PBS. This method removed approximately 90% of surface-bound Tf in TRVb-TfR2α cells.

Efflux of Tf from cells

Cells, plated at a density of 1×10^6 cells/well in 35-mm six-well plates 24 h before the experiments, were preincubated with F-12 three times for 10 min at 37 °C, chilled on ice for 30 min, and then incubated with F-12 containing 2% BSA and 3.5×10^{-7} M ^{125}I-labeled Tf for 60 min at 37 °C. After acid washing, fresh F-12 medium was added, and cells were again incubated at 37 °C. At indicated times, F-12 media were collected, and cells were washed with ice-cold PBS and solubilized by 0.1% Triton X-100. Media and cell lysates were then taken for γ-counting. After counting, media were incubated with 10% TCA/2% PTA for 30 min on ice, and then centrifuged at 14,000 rpm in an Eppendorf centrifuge for 20 min. Tf degradations were calculated from the radioactivities of supernatants and precipitates.

Pulse-chase study

TRVb-TfR2α cells were incubated with 5.1×10^{-7} M [^{125}I]Tf, as previously described, for 1 h at 4 °C. Cells were then washed with ice-cold PBS five times. Fresh F-12 medium was added, and cells were incubated at 37 °C. At indicated times, cells were chilled on ice, and media were immediately collected. Cells were again washed with ice-cold PBS, and media were collected. Cells were then acid washed to quantify surface-bound Tf and solubilized for the measurement of intracellular Tf.

Immunoprecipitation–Western blot analysis

Human-hepatoma-derived HuH-7 cells were transiently transfected with the TfR2α expression vector, as described above. At 48 h after transfection, 5×10^6 cells were washed with PBS five times and collected with a cell scraper. Harvested cells were dissolved in 40 μl of the cell extraction buffer of the Mammalian Cell Extraction Kit (BioVision Incorporated, Mountain View, CA) following the manufacturer's instructions for Western blot analysis without immunoprecipitation, or in 1.5 ml of lysis buffer [10 mM Tris–HCl, 150 mM NaCl, 1% Nonidet P-40, 1 mM ethylenediaminetetraacetic acid, and 1 mM PMSF containing 1:2000 Protease Inhibitor Cocktail (Boehringer-Mannheim; pH 7.4)] for immunoprecipitation–Western blot analysis. Freezing and thawing were performed three times, following which samples were centrifuged at 2700*g*. Protein G Sepharose (Amersham Biosciences, Uppsala, Sweden) was added, and preparations were incubated at 4 °C for 8 h, then centrifuged at 1500*g* for 5 min. Supernatants were then collected for incubation with anti-FLAG M2 antibody (Sigma), which recognizes FLAG at any location in the target protein, or with anti-TfR1 antibody (Zymed Laboratory, South San Francisco, CA) for 8 h at 4 °C. Protein G Sepharose was added, and incubation continued for an additional 8 h at 4 °C. Samples were centrifuged at 1500*g* for 5 min, and pellets were washed with PBS five times. Concentrated dye buffer was added, and final concentrations were adjusted to 10 mM Tris–HCl, 1 mM ethylenediaminetetraacetic acid, 2.5% SDS, 5% β-mercaptoethanol, and 0.01% bromophenol blue (pH 8.0). Samples were then immersed in boiling water for 5 min and centrifuged at 20,000*g* for 5 min to remove precipitated material. Electrophoresis using a 12% gradient polyacrylamide gel and transfer to a nitrocellulose membrane were carried out. The membrane was incubated with anti-TfR2 antibody (9F8 1C11) (Santa Cruz Biotechnology, Inc., Santa Cruz, CA) diluted 1:200 or with anti-TfR1 antibody diluted 1:1000, and then with horseradish-peroxidase-conjugated goat anti-mouse IgG antibody (R&D Systems, Minneapolis,

MN) diluted 1:2000. SuperSignal West Pico Chemiluminescent Substrate (Thermo Scientific, Rockford, IL) was used as development substrate.

Atomic force microscopy

The details of the methods for investigation using AFM were previously reported.[15] In brief, the probe of AFM is a sharp tip placed at the end of a soft cantilever. A piezoelectric scanner allows the precise positioning of the tip relative to the sample. A laser beam reflected on the cantilever backside and detected by photodiodes is used to measure cantilever deflection. This signal is either used as feedback to control the scanner (imaging mode) or measured and converted into force (force spectroscopy mode). Since the cantilever is mounted under the scanner, the optical path is free, and AFM can be coupled to an optical microscope. Tf was linked to the AFM tip by a three-step functionalizing protocol. First, SiN tips are aminosilanized by exposure to APTES vapors. Second, a heterobifunctional polyethylene glycol linker is anchored to amino-group-bearing tips through its NHS end. Third, Tf is attached to the polyethylene glycol linker free end via a maleimide–cysteine bond.

Measuring the interaction force between Tf and TfR2α by AFM

HLF cells (human hepatoma) were cotransfected with TfR2α and GFP for identification, as previously described.[33] A Tf-coated tip was brought in contact with the cell surface, allowing the proteins to bind. The tip was then retracted, resulting first in protein stretching, then unbinding. Cantilever deflections during one cycle are recorded in a force curve. A binding–unbinding event between Tf and TfR2α is represented by a sawtooth pattern on the curve. It allows calculation of the force necessary to unbind the two proteins, using the cantilever spring constant (Hooke's law). The mean unbinding force is obtained by fitting a Gaussian curve to the force histogram. The error on the mean unbinding force is calculated by adding the standard deviation of the sample and the error resulting from the spring constant calibration (10%). Moreover, the unbinding force is related to the pulling rate by:

$$F^* = \frac{k_B T}{x} \ln\left(\frac{x}{k_0 k_B T}\right) + \frac{k_B T}{x} \ln(r_f)$$

where F^* is the most probable unbinding force, k_0 is the dissociation rate constant, r_f is the loading rate applied, x is the width of the energy barrier along the direction of the applied force, k_B is the Boltzmann constant, and T is temperature.

Acknowledgements

We are grateful to Dr. Timothy E. McGraw for providing the CHO TRVb cells used in this study. This work was supported, in part, by grants 1 PO1 DK55495 and 5 RO1 DK015056 from the National Institutes of Health, US Public Health Service, USA.

Supplementary Data

Supplementary data associated with this article can be found, in the online version, at doi:10.1016/j.jmb.2010.01.026

References

1. Kühn, L. C., McClelland, A. & Ruddle, F. H. (1984). Gene transfer, expression, and molecular cloning of the human transferrin receptor gene. *Cell*, **37**, 95–103.
2. Feder, J. N., Gnirke, A., Thomas, W., Tsuchihashi, Z., Ruddy, D. A., Basava, A. *et al.* (1996). A novel MHC class I-like gene is mutated in patients with hereditary haemochromatosis. *Nat. Genet.* **13**, 399–408.
3. Feder, J. N., Penny, D. M., Irrinki, A., Lee, V. K., Lebrón, J. A., Watson, N. *et al.* (1998). The hemochromatosis gene product complexes with the transferrin receptor and lowers its affinity for ligand binding. *Proc. Natl Acad. Sci. USA*, **95**, 1472–1477.
4. Lebrón, J. A., Bennett, M. J., Vaughn, D. E., Chirino, A. J., Snow, P. M., Mintier, G. A. *et al.* (1998). Crystal structure of the hemochromatosis protein HFE and characterization of its interaction with transferrin receptor. *Cell*, **93**, 111–123.
5. Waheed, A., Parkkila, S., Zhou, X. Y., Tomatsu, S., Tsuchihashi, Z., Feder, J. N. *et al.* (1997). Hereditary hemochromatosis: effects of C282Y and H63D mutations on association with β2-microglobulin, intracellular processing, and cell surface expression of the HFE protein in COS-7 cells. *Proc. Natl Acad. Sci. USA*, **94**, 12384–12389.
6. Roy, C. N., Penny, D. M., Feder, J. N. & Enns, C. A. (1999). The hereditary hemochromatosis protein, HFE, specifically regulates transferrin-mediated iron uptake in HeLa cells. *J. Biol. Chem.* **274**, 9022–9028.
7. Gunshin, H., Mackenzie, B., Berger, U. V., Gunshin, Y., Romero, M. F., Boron, W. F. *et al.* (1997). Cloning and characterization of a mammalian proton-coupled metal-ion transporter. *Nature*, **388**, 482–488.
8. Fleming, M. D., Romano, M. A., Su, M. A., Garrick, L. M., Garrick, M. D. & Andrews, N. C. (1998). Nramp2 is mutated in the anemic Belgrade (b) rat: evidence of a role for Nramp2 in endosomal iron transport. *Proc. Natl Acad. Sci. USA*, **95**, 1148–1153.
9. Gruenheid, S., Canonne-Hergaux, F., Gauthier, S., Hackam, D. J., Grinstein, S. & Gros, P. (1999). The iron transport protein NRAMP2 is an integral membrane glycoprotein that colocalizes with transferrin in recycling endosomes. *J. Exp. Med.* **189**, 831–841.
10. Klausner, R. D., Van Renswoude, J., Ashwell, G., Kempf, C., Schechter, A. N., Dean, A. & Bridges, K. R. (1983). Receptor-mediated endocytosis of transferrin in K562 cells. *J. Biol. Chem.* **258**, 4715–4724.
11. Dautry-Varsat, A., Ciechanover, A. & Lodish, H. F. (1983). pH and the recycling of transferrin during receptor-mediated endocytosis. *Proc. Natl Acad. Sci. USA*, **80**, 2258–2262.
12. Ciechanover, A., Schwartz, A. L., Dautry-Varsat, A. & Lodish, H. F. (1983). Kinetics of internalization and recycling of transferrin and the transferrin receptor in a human hepatoma cell line. Effect of lysosomotropic agents. *J. Biol. Chem.* **258**, 9681–9689.
13. Kawabata, H., Yang, R., Hirama, T., Vuong, P. T., Kawano, S., Gombart, A. F. & Koeffler, H. P. (1999). Molecular cloning of transferrin receptor 2. A new member of the transferrin receptor-like family. *J. Biol. Chem.* **274**, 20826–20832.

14. Kawabata, H., Germain, R. S., Vuong, P. T., Nakamaki, T., Said, J. W. & Koeffler, H. P. (2000). Transferrin receptor 2-alpha supports cell growth both in iron-chelated cultured cells and *in vivo*. *J. Biol. Chem.* **275**, 16618–16625.
15. Yersin, A., Osada, T. & Ikai, A. (2008). Exploring transferrin–receptor interactions at the single-molecule level. *Biophys. J.* **94**, 230–240.
16. Chan, R. Y., Ponka, P. & Schulman, H. M. (1992). Transferrin-receptor-independent but iron-dependent proliferation of variant Chinese hamster ovary cells. *Exp. Cell Res.* **202**, 326–336.
17. Lawrence, C. M., Ray, S., Babyonyshev, M., Galluser, R., Borhani, D. W. & Harrison, S. C. (1999). Crystal structure of the ectodomain of human transferrin receptor. *Science*, **286**, 779–782.
18. Fleming, R. E., Migas, M. C., Holden, C. C., Waheed, A., Britton, R. S., Tomatsu, S. *et al.* (2000). Transferrin receptor 2: continued expression in mouse liver in the face of iron overload and in hereditary hemochromatosis. *Proc. Natl Acad. Sci. USA*, **97**, 2214–2219.
19. Trinder, D., Zak, O. & Aisen, P. (1996). Transferrin receptor-independent uptake of diferric transferrin by human hepatoma cells with antisense inhibition of receptor expression. *Hepatology*, **23**, 1512–1520.
20. Sasaki, K., Zak, O. & Aisen, P. (1993). Antisense suppression of transferrin receptor gene expression in a human hepatoma cell (HuH-7) line. *Am. J. Hematol.* **42**, 74–80.
21. McGraw, T. E., Greenfield, L. & Maxfield, F. R. (1987). Functional expression of the human transferrin receptor cDNA in Chinese hamster ovary cells deficient in endogenous transferrin receptor. *J. Cell Biol.* **105**, 207–214.
22. West, A. P., Jr., Bennett, M. J., Sellers, V. M., Andrews, N. C., Enns, C. A. & Bjorkman, P. J. (2000). Comparison of the interactions of transferrin receptor and transferrin receptor 2 with transferrin and the hereditary hemochromatosis protein HFE. *J. Biol. Chem.* **275**, 38135–38138.
23. Dubljevic, V., Sali, A. & Goding, J. W. (1999). A conserved RGD (Arg-Gly-Asp) motif in the transferrin receptor is required for binding to transferrin. *Biochem. J.* **341**, 11–14.
24. Osterloh, K. & Aisen, P. (1989). Pathways in the binding and uptake of ferritin by hepatocytes. *Biochim. Biophys. Acta*, **1011**, 40–45.
25. Ikuta, K., Fujimoto, Y., Suzuki, Y., Tanaka, K., Saito, H., Ohhira, M. *et al.* (2000). Overexpression of hemochromatosis protein, HFE, alters transferrin recycling process in human hepatoma cells. *Biochim. Biophys. Acta*, **1496**, 221–231.
26. Levy, J. E., Jin, O., Fujiwara, Y., Kuo, F. & Andrews, N. C. (1999). Transferrin receptor is necessary for development of erythrocytes and the nervous system. *Nat. Genet.* **21**, 396–399.
27. Camaschella, C., Roetto, A., Cali, A., De Gobbi, M., Garozzo, G., Carella, M. *et al.* (2000). The gene TFR2 is mutated in a new type of haemochromatosis mapping to 7q22. *Nat. Genet.* **25**, 14–15.
28. Roetto, A., Totaro, A., Piperno, A., Piga, A., Longo, F., Garozzo, G. *et al.* (2001). New mutations inactivating transferrin receptor 2 in hemochromatosis type 3. *Blood*, **97**, 2555–2560.
29. McFarlane, A. S. (1963). *In vivo* behavior of I-fibrinogen. *J. Clin. Invest.* **42**, 346–361.
30. Young, S. P. & Aisen, P. (1980). The interaction of transferrin with isolated hepatocytes. *Biochim. Biophys. Acta*, **633**, 145–153.
31. Zak, O., Trinder, D. & Aisen, P. (1994). Primary receptor-recognition site of human transferrin is in the C-terminal lobe. *J. Biol. Chem.* **269**, 7110–7114.
32. Klotz, I. M. & Hunston, D. L. (1971). Properties of graphical representations of multiple classes of binding sites. *Biochemistry*, **10**, 3065–3069.
33. Yersin, A., Hirling, H., Kasas, S., Roduit, C., Kulangara, K., Dietler, G. *et al.* (2007). Elastic properties of the cell surface and trafficking of single AMPA receptors in living hippocampal neurons. *Biophys. J.* **92**, 4482–4489.

DOI 10.1002/prca.200900112 *Proteomics Clin. Appl.* 2009, *3*, 1256–1264

RESEARCH ARTICLE

Heterogeneous expressions of hepcidin isoforms in hepatoma-derived cells detected using simultaneous LC-MS/MS

Takaaki Hosoki[1], Katsuya Ikuta[1], Yasushi Shimonaka[2], Yusuke Sasaki[2], Hideyuki Yasuno[2], Kazuya Sato[1], Takaaki Ohtake[1], Katsunori Sasaki[3], Yoshihiro Torimoto[4], Keiji Saito[2] and Yutaka Kohgo[1]

[1] Division of Gastroenterology and Hematology/Oncology, Department of Medicine, Asahikawa Medical College, Asahikawa, Japan
[2] Kamakura Research Labs, Chugai Pharmaceutical Co., Ltd., Kamakura, Japan
[3] Department of Gastrointestinal Immunology and Regenerative Medicine, Asahikawa Medical College, Asahikawa, Japan
[4] Oncology Center, Asahikawa Medical College Hospital, Asahikawa, Japan

Received: June 3, 2009
Revised: July 13, 2009
Accepted: July 17, 2009

Hepcidin, a key regulator of iron homeostasis, is known to have three isoforms: hepcidin-20, -22, and -25. Hepcidin-25 is thought to be the major isoform and the only one known to be involved in iron metabolism; the physiological roles of other isoforms are poorly understood. Because of its involvement in the pathophysiology of hereditary hemochromatosis and the anemia of chronic disease, the regulatory mechanisms of hepcidin expression have been extensively investigated, but most studies have been performed only at the transcriptional level. Difficulty in detecting hepcidin has impeded *in vitro* research. In the present study, we developed a novel method for simultaneous quantification of hepcidin-20, -22, and -25 in the media from hepatoma-derived cell lines. Using this method, we determined the expression patterns of hepcidin isoforms and the patterns of responses to various stimuli in human hepatoma-derived cultured cells. We found substantial differences among cell lines. In conclusion, a novel method for simultaneous quantification of hepcidin isoforms is presented. Heterogeneous expressions of hepcidin isoforms in human hepatoma-derived cells were revealed by this method. We believe our method will facilitate quantitative investigation of the role hepcidin plays in iron homeostasis.

Keywords:
Hepatocyte / Hepcidin antimicrobial peptide / Iron metabolism / LC-MS/MS

Correspondence: Dr. Katsuya Ikuta, Division of Gastroenterology and Hematology/Oncology, Department of Medicine, Asahikawa Medical College, 2-1-1-1 Midorigaoka-Higashi, Asahikawa, Hokkaido 078-8510, Japan
E-mail: ikuta@asahikawa-med.ac.jp
Fax: +81-166-68-2469

Abbreviations: **Ct,** threshold cycle; **DFO,** desferrioxamine; **EMEM,** Eagle's minimum essential medium; **FAC,** ferric ammonium citrate; **HAMP,** hepcidin antimicrobial peptide; **holo-Tf,** holo-transferrin; **IL-1β,** interleukin-1β; **IL-6,** interleukin-6; **LPS,** lipopolysaccharide; **QC,** quality control; **qRT-PCR,** quantitative RT-PCR; **SRM,** selected reaction monitoring

1 Introduction

Hepcidin is a small peptide mainly produced by the liver, and it is thought to be the key regulator in iron homeostasis [1, 2]. Hepcidin binds to ferroportin, the mammalian iron exporter expressed on the basolateral side of enterocytes and on the cell surface of macrophages, thereby causing the internalization and degradation of ferroportin [3]. Hepcidin thus inhibits iron uptake from the gastrointestinal tract and iron release from reticuloendothelial cells, so that iron balance of the body is negatively regulated by hepcidin [1, 2]. Increased

hepcidin expression therefore leads to iron deficiency while decreased hepcidin expression causes iron overload.

Hepcidin is involved in several diseases, such as hereditary hemochromatosis and the anemia of chronic disease. In hereditary hemochromatosis, various mutations occur in genes such as *HFE*, *hemojuvelin*, and *transferrin receptor 2*, leading to decreased hepcidin expression despite generalized iron overload [4–6]. In contrast, in anemia of chronic disease, inflammatory cytokines such as interleukin-6 (IL-6) [7, 8] and interleukin-1β (IL-1β) [9, 10] upregulate hepcidin expression and thus cause iron-deficiency anemia.

Recently, the regulation of hepcidin expression has been intensively studied to reveal pathophysiological mechanisms involved in diseases in which iron metabolism is altered. For instance, the cytokine IL-6 increases hepcidin synthesis utilizing signal transducers and activators of transcription-3 during inflammation such as caused by systemic infections [11]. The bone morphogenic proteins (BMPs) are members of the transforming growth factor β superfamily, and BMPs have been proposed to be involved in hemojuvelin-mediated regulation of hepcidin synthesis [12]. However, almost all research on the regulation of hepcidin expression has been restricted to studying changes in transcription of the *hepcidin antimicrobial peptide* (*HAMP*) gene utilizing RT-PCR under various conditions.

Hepcidin is produced mainly by hepatocytes expressing the *HAMP* gene located on chromosome 19. The transcript of this gene is believed to produce a prepropeptide of 84 amino acids, and then the peptide is digested by furin, the intercellular convertase, and finally the mature form of hepcidin appears in the peripheral blood [13]. However, there is little information about the ratios of serum prohepcidin to mature hepcidin, and the secreted fraction of hepcidin to hepcidin retained intracellularly. In addition, kidney cells have been shown to produce hepcidin independently of the liver [14]. Therefore, there is no proof that *HAMP* transcript levels of the liver reflect total body secretion of hepcidin-25. Consequently, it is desirable that hepcidin be determined from peptide levels in the serum, in addition to transcriptional levels of the liver and other organs.

Three isoforms of mature hepcidin are known. A 25-amino acid peptide (hepcidin-25) is thought to be the major isoform [15], but other forms of hepcidin such as hepcidin-20 and -22 have been detected in human urine [16]. Only hepcidin-25 has been shown to cause the internalization and degradation of ferroportin. However, the possibility arises that hepcidin-20 and -22 have different physiological roles in homeostasis and their expressions are regulated independently from hepcidin-25. It is therefore desirable that hepcidin-20, -22, and -25 be separately quantified.

The first method for measuring prohepcidin, using ELISA, was reported by Kulaksiz *et al.* [17]. That method has been applied for the analysis of hepcidin expression levels, but there is little information about how and whether hepatocytes secrete prohepcidin into the blood [17]. Several groups have developed antibodies to detect and measure hepcidin, but difficulties for differentiation of hepcidin-20, -22, and -25 [18] persist. MS-based modalities have been used in recent years for measuring hepcidin. For instance, SELDI-TOF-MS has been used for semi-quantification [19, 20], and LC-MS/MS has been employed for quantification of hepcidin [21, 22]. These methods are applicable to assaying clinical samples such as blood and urine. Most recently, Ganz *et al.* reported development of an ELISA system for quantification of human serum hepcidin that is expected to be a powerful tool for clinical samples [23].

Experiments *in vitro* would also be valuable for investigating the complex molecular mechanisms regulating hepcidin expression. Detection and quantification of hepcidin in cell culture media has been difficult, probably due to its low concentration.

We therefore aimed to develop a sensitive new method for measuring hepcidin that can simultaneously measure hepcidin-20, -22, and -25 secreted in culture media by hepatoma-derived cells. We now report such a method, improving the MS-based modality that we previously reported [22]. We also determined the characteristics of hepcidin expression of various hepatoma cell lines using the new method, which can be applied to analyzing differences among hepatoma cells of varying lineage.

2 Materials and methods

2.1 Hepcidin standards

Human hepcidin-25 was obtained from the Peptide Institute (Osaka, Japan). Hepcidin-20, -22, and [$^{13}C_{18}$, $^{15}N_3$]-hepcidin-25 were synthesized at the Peptide Institute.

2.2 Chemicals

BMP2 and holo-transferrin (holo-Tf) were purchased from R & D Systems; IL-6 was obtained from Wako Pure Chemical Industries, Osaka, Japan. FBS was purchased from Japan Bioserum; Eagle's minimum essential medium (EMEM), DMEM, RPMI-1640 medium, L-glutamine, and sodium bicarbonate were purchased from Sigma-Aldrich. Penicillin–streptomycin solution were bought from Invitrogen. IL-1β was purchased from Wako Pure Chemical Industries; desferrioxamine (DFO), ferric ammonium citrate (FAC), lipopolysaccharide (LPS), and cobalt chloride were obtained from Sigma-Aldrich. Decanoyl-RVKR-CMK (furin inhibitor I) was purchased from Calbiochem (Darmstadt, Germany). All other chemicals and solvents were of analytical reagent grade.

2.3 Cell cultures

Human hepatoma-derived cell lines used in this study were HepG2, HuH-1, HuH-2, HuH-4, HuH-6, HuH-7, WRL68, HB611, Hep3B, HLE, HLF, SK-HEP-1, and human primary

hepatocytes derived from normal liver (Applied Cell Biology Research Institute).

HuH-4, HB611, and HuH-6 cells were incubated with RPMI1640; HuH-7 cells were incubated with DMEM. Other cells were incubated with EMEM. Those medium were supplemented with 10% FBS, 100 U/mL penicillin, and 100 μg/mL streptomycin. All cells were cultured at 37°C in a humidied incubator with 5% CO_2. In some experiments, FBS-free UltraCulture medium (Lonza, MD, USA) supplemented with 2 mM L-glutamine was used. HepG2 cells could survive in this serum-free medium for more than 3 days.

Cells at the density of 1×10^6 cells/mL were grown in 6-well plates for 24 h to almost 80% conuency in 2 mL of culture medium. Medium in each well was replaced by 2 mL of culture medium containing various stimulants and then incubated for 48 h. All cell lines were maintained with 20 ng/mL IL-6 or 30 μM holo-Tf or no additives for control cells.

After 48 h, culture media were collected and analyzed for hepcidin-20, -22, and -25 concentrations as follows: 50 μL of 4% trichloroacetic acid solution containing 200 ng/mL [$^{13}C_{18}$, $^{15}N_3$]-hepcidin-25 as internal standard was added to an equal amount of each culture medium, mixed vigorously, and centrifuged. A 20-μL aliquot of the resulting supernatant was analyzed quantitatively by LC-MS/MS. Cells were lysed with 0.1% Triton X-100 for protein assay, or by Sepazol™ (Nacarai Tesque, Japan) for RT-PCR studies.

HepG2 cells were also treated with various reagents instead of IL-6 or holo-Tf, such as 200 pg/mL IL-1β, 100 μM DFO, 100 μM FAC, 1 μg/mL LPS, 50 μM $CoCl_2$, or 50 μM furin inhibitor I. After 48 h, culture media were collected for quantification of hepcidin isoforms, and cells were lysed for measuring protein concentrations.

Each treatment was performed in triplicate, and data presented as mean and SD.

2.4 LC/ESI-MS/MS analysis

LC/ESI-MS/MS was performed using an API4000QTRAP (Applied Biosystems, Foster City, CA, USA) equipped with a UPLC ACQUITY™ systems (Waters). The turboionspray was operated in the positive ion mode at 5500 V for the ion spray voltage. Analytical chromatography of human hepcidin-20, -22, and -25 was accomplished on a PLRP-S column (5 μm, 300 Å, 150 mm × 2.0 mm id; Polymer Laboratories, Shropshire, UK). Instrument control and data processing were with Analyst™ software version 1.4 (Applied Biosystems).

2.5 Quantitative analysis of human hepcidin-20, -22, and -25

Selected reaction monitoring (SRM) transitions were as follows: human hepcidin-20, m/z 548.85 → 119.80; human hepcidin-22, m/z 610.14 → 119.80; human hepcidin-25, m/z 558.80 → 120.07; [$^{13}C_{18}$, $^{15}N_3$]-human hepcidin-25, m/z 563.11 → 109.60. The declustering potential for human hepcidin-20, -22, -25, and [$^{13}C_{18}$, $^{15}N_3$]-human hepcidin-25 were 50, 50, 81, and 81 V, respectively. The turboionspray source was maintained at a temperature of 600°C. Collision energies for human hepcidin-20, -22, -25, and [$^{13}C_{18}$, $^{15}N_3$]-human hepcidin-25 were 52, 59, 73 and 75 V, respectively. The collisional activation dissociation gas was set at 4. Mobile phase A was 0.1% aqueous formic acid, and mobile phase B was 0.1% formic acid in ACN. Gradient conditions were as follows: B 20% (0 min, 0.3 mL/min) → 20% (2.01 min, 0.3 mL/min) → 25% (5.00 min, 0.3 mL/min) → 25% (10.00 min, 0.3 mL/min) → 90% (10.01 min, 0.3 mL/min) → 90% (12.00 min, 0.3 mL/min) → 20% (12.01 min, 0.3 mL/min) → 20% (14.00 min, 0.3 mL/min).

Analysis of hepcidin-25 in the BMP2-stimulated HepG2 culture medium was performed on the 6520 quadrupole-TOF/MS (Agilent Technologies).

2.6 RNA isolation and quantitative RT-PCR

Total RNA was isolated and quantitative RT-PCR (qRT-PCR) was performed in a reaction mix containing TaqMan Universal PCR Master Mix No AmpErase UNG (Applied Biosystems), specific human *HAMP* primers, and probe (pre-validated Taqman gene expression assay, Applied Biosystems), and 100 ng of cDNA. All reactions were multiplexed with the housekeeping gene 18S, provided as a pre-optimized control probe (Applied Biosystems) enabling data to be expressed as delta threshold cycle (ΔCt) values (where ΔCt = Ct of 18 s subtracted from Ct of gene of interest). Reactions were as follows: 50°C for 2 min, 95°C for 10 min; then 60 cycles of 95°C for 15 s and 60°C for 1 min. All measurements were performed in triplicate, and relative *HAMP* mRNA expression was expressed as fold expression over the average of *HAMP* mRNA expression corresponding to the HepG2 cells.

2.7 Cellular protein assay

Cell were lysed with 0.1% Triton-X and total protein concentrations were determined using the Bradford reagent (BioRad, Hercules, CA, USA), following the manufacturer's instructions.

3 Results

3.1 Establishment of quantitative measurement of hepcidin isoforms

To improve further the method for quantifying small peptides by LC-MS/MS, we developed a quantitative and simultaneous method for hepcidin-20, -22, and -25 in

biological fluids. Upon optimization of SRM conditions, the most intense precursor ions were selected in each mass spectrum to detect hepcidin isoforms. Product ions were selected to maximize sensitivity and selectivity. Using EMEM supplemented with 10% FBS as matrix, various concentrations of synthetic hepcidin isoforms were spiked, and analyzed by LC-MS/MS. Isoform peaks were not interfered with by a blank matrix, indicating the method has good selectivity.

Our method was validated by specificity, linearity, lower limit of quantification, intra-assay precision, and accuracy. Calibration curves were constructed over the range 2–1000 ng/mL in the above matrix. Five replicates of 2, 5, 50, 500, and 1000 ng/mL of each isoform quality control (QC) samples were prepared and analyzed by LC-MS/MS.

There was no interference peak at retention time of each isoform, confirming good specificity (Fig. 1A). Linearity of the calibration curves by weighted ($1/x^2$) linear regression was excellent (correlation coefficient: $r = 0.9974$ for hepcidin-20, $r = 0.9937$ for hepcidin-22, $r = 0.9950$ for hepcidin-25; Fig. 1B). Accuracies of the back-corrected concentrations were within 87.4–109% for hepcidin-20, 80.1–110% for hepcidin-22, and 80.5–109% for hepcidin-25. The lower limits of quantification for each hepcidin isoform was 2 ng/mL. Coefficients of variance in intra-assay QC samples were 1.2–8.6% for hepcidin-20, 3.1–5.7% for hepcidin-22, and 1.5–7.0% for hepcidin-25. Accuracies for QC samples were 99.7–122.1% for hepcidin-20, 102.6–132.5% for hepcidin-22, and 99.1–141.2% for hepcidin-25. These results indicate that the method is adequate for quantifying hepcidin isoforms in culture media.

3.2 Detection of hepcidin isoforms in HepG2 media

In the SRM chromatogram of HepG2 medium analyzed by LC-MS/MS, peaks corresponding to the retention time of synthetic hepcidin-22 and -25, but not hepcidin-20, were detected. Peaks corresponding to hepcidin-22 and -25 were also detected and up-regulated in 100 ng/mL BMP2 stimulated HepG2 medium (Fig. 2A). No peaks corresponding to hepcidin-20 were founded in the chromatogram of HepG2 media at any tested conditions.

We tried to identify the component of the corresponding peak for hepcidin-25 in HepG2 medium. For that purpose, BMP2 medium was prepared because it contained a relatively high concentration of putative hepcidin-25, (65.9 ng/mL). Synthetic hepcidin-25 and BMP2 medium were analyzed by quadrupole-TOF/MS. The major precursor ions of synthetic hepcidin-25 ranged from $m/z = 558.4$–559.0. At the same retention time, precursor ions from BMP2 medium showed a similar distribution (Fig. 2B). Mass spectra of product ions were also similar. Several major common product ions were observed (Fig. 2C). Overall, synthetic hepcidin-25 and HepG2-derived peak components are similar in retention time and mass spectra of the

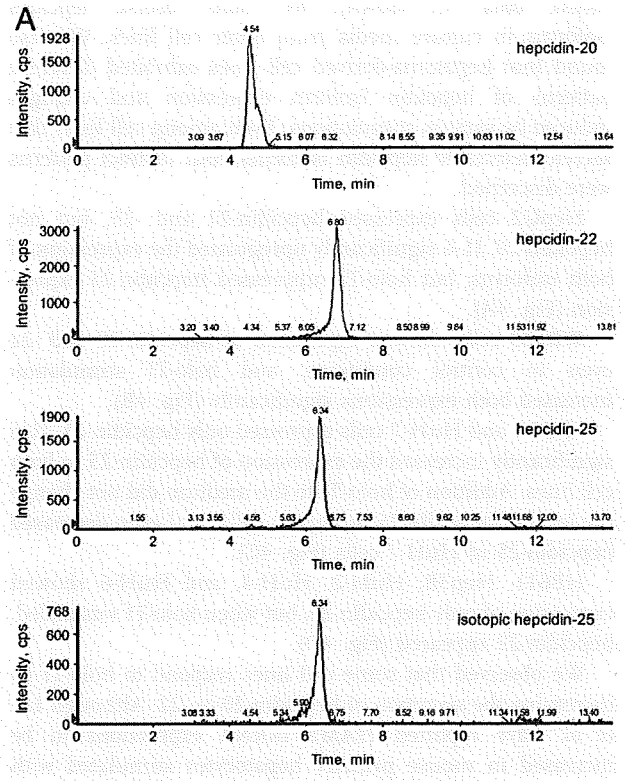

Figure 1. (A) Representative LC-MS/MS chromatograms of hepcidin-20, -22, -25, and blank isotopic hepcidin-25 sample. (B) The calibration curves of hepcidin-20, -22, and -25 in the culture medium are linear in the range of 2–1000 ng/mL. The correlation coefficients of calibration curves are as follows: hepcidin-20, $r = 0.9974$; hepcidin-22, $r = 0.9937$; hepcidin-25, $r = 0.9950$.

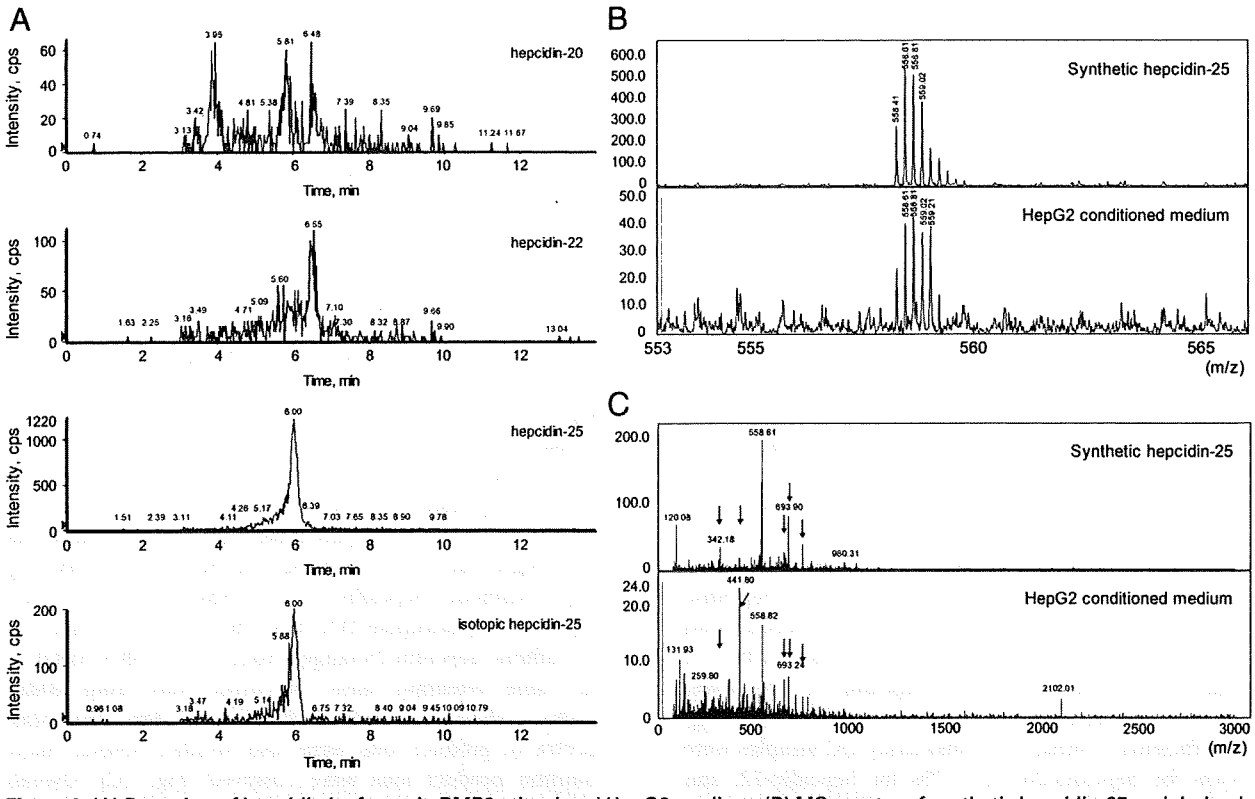

Figure 2. (A) Detection of hepcidin isoforms in BMP2-stimulated HepG2 medium. (B) MS spectra of synthetic hepcidin-25 and derived peak from BMP2-stimulated HepG2 medium showing similar patterns. (C) MS/MS spectra of synthetic hepcidin-25 and derived peak from BMP2-stimulated HepG2 medium showing similar patterns. Arrows show common fragments.

precursor ions and product ions, verifying that the peak detected in the culture medium represents hepcidin-25.

3.3 HAMP gene expressions in hepatoma-derived cell lines

We aimed at first to determine qualitatively whether cell lines derived from hepatocellular carcinomas express the *HAMP* gene as assayed by RT-PCR. Expression levels of *HAMP* mRNA differed among cell lines (Fig. 3A). HepG2, HuH-1, and HuH-7 cells showed relatively high *HAMP* mRNA expressions, but other cells exhibited only slight expressions. qRT-PCR was then performed (Fig. 3B). HepG2, HuH-1, and HuH-7 cells expressed high levels of *HAMP* mRNA, compatible with the results of qualitative RT-PCR. Only slight or moderate *HAMP* mRNA expression was found in other cells.

3.4 Quantification of hepcidin isoforms in the culture medium of various hepatoma-derived cell lines

HLE, HLF, SK-Hep1, and human primary hepatocytes did not show any detectable hepcidin isoforms in their culture media (data not shown). We could observe hepcidin isoforms in culture media from other cell lines. We also found that hepatoma-derived cell lines exhibited different patterns of hepcidin isoform expression and changes induced by various stimulations. Even among cell lines that secrete detectable hepcidin isoforms, four distinct patterns were discerned.

HepG2 cells expressed hepcidin-22 and -25, but not hepcidin-20. IL-6 significantly upregulated the expression of both isoforms, but holo-Tf suppressed hepcidin-25 expression (Fig. 4A).

WRL68 cells showed expression of hepcidin-20 and -22 even in control conditions, and holo-Tf stimulation increased both expressions significantly (Fig. 4B).

HuH-1 and HuH-7 cells expressed only hepcidin-25. IL-6 significantly increased the expression of hepcidin-25 in both cell lines. Addition of holo-Tf to the medium did not change the level of hepcidin-25 in HuH-1 cells, and even decreased hepcidin-25 in HuH-7 cells (Fig. 4C).

HB611, Hep3B, HuH-2, HuH-4, and HuH-6 showed expression of only hepcidin-20, but when holo-Tf was added, hepcidin-22 appeared (Fig. 4D).

We observed that some cell lines respond to holo-Tf by increasing the secretion of hepcidin-20 or -22. Although Lin *et al.* have reported *HAMP* mRNA expressions to be increased in mouse primary hepatocytes stimulated with

